Polym. Korea, Vol. 50, No. 5, pp. 663-670 (2026)
https://doi.org/10.7317/pk.2026.50.5.663
ISSN 2234-8077(Online)

갈대 유래 셀룰로오스 아세테이트의 제조 및 특성

Chunxiang Wang*,**,***, Kaifang Xie*,**,***,†, Jinzhao Zhang*,**,***, Xiaokang Wang*,**,***
Hengshu Zhou*,**,***, Haizhe Tang*,**,***, Changwei Liu*,**,***, and Bokun Lin*,**,***
*College of Textile and Fashion, Hunan Institute of Engineering
**Engineering Technology Research Center of New Fiber Fabric and Processing, Hunan Institute of Engineering
***Key Laboratory of Intelligent Textile Processing Technology, College of Hunan Province
(2024년 4월 15일 접수, 2026년 7월 2일 수정, 2026년 7월 29일 채택)

Preparation and Properties of Reed-based Cellulose Acetate

Chunxiang Wang*,,***, Kaifang Xie*,**,***,†, Jinzhao Zhang*,**,***, Xiaokang Wang*,**,***,**
Hengshu Zhou*,,***, Haizhe Tang*,**,***, Changwei Liu*,**,***, and Bokun Lin*,**,*****
**College of Textile and Fashion, Hunan Institute of Engineering, No. 88 East Fuxing Road, Yuetang District, Xiangtan, 411104, China*
***Engineering Technology Research Center of New Fiber Fabric and Processing, Hunan Institute of Engineering, Xiangtan, Hunan 411104, China*
****Key Laboratory of Intelligent Textile Processing Technology, College of Hunan Province, Xiangtan, Hunan 411104, China*
(Received April 15, 2024; Revised July 2, 2026; Accepted July 29, 2026)

Abstract: To explore the feasibility of preparing cellulose acetate (CA) from reed, this study used self-made triarrhena lutarioriparia dissolving pulp as raw material and conducts orthogonal experiments using homogeneous reaction method. The apparent morphology, chemical and crystal structure, thermal stability of CA are measured. When acetic anhydride dosage, reaction temperature and activation time were 60 mL, 70 °C and 40 min respectively, the performance of CA was optimal with whiteness of 84.24, the degree of polymerization (DP) was 172, and the degree of substitution (DS) was 2.61. The hydroxyl groups in the cellulose macromolecular chain are substituted by acetyl groups, and the reaction product exhibits typical Fourier transform infrared spectroscopy (FTIR), X-ray diffraction (XRD), proton nuclear magnetic resonance spectroscopy (^{1}H NMR) curves of CA. The destruction of the cellulose's stable structure leads to a decrease in the degree of crystallinity and thermal stability of CA, with the highest rate of weight loss occurring at 255 °C. The successful preparation of reed-based CA lays a good research foundation for acetate fiber spinning.

Keywords: reed, triarrhena lutarioriparia dissolving pulp, cellulose acetate, acetylation reaction, whiteness, degree of polymerization, degree of substitution.

Introduction

Reed is a renewable herbaceous plant that grows widely in marshes, wetlands, lake shores, river banks, etc. In the Dongting Lake region of Hunan Province, the annual production of reed can reach more than 900000 tons, which is mostly used in the paper industry.[1] However, due to environmental protection requirements, many paper mills were shut down, resulting in large-scale abandonment of reed and causing a series of ecological, economic and livelihood issues. Therefore, it is necessary to develop various ways to utilize the surplus reed resources, such as building insulation materials,[2] bioethanol,[3] edible mushrooms,[4] industrial enzymes,[5] eco-boards, biochar etc. If reeds can be converted into high-value regenerated cellulose fibers (such as modal fibers, Lyocell fibers, acetate fibers, etc.) and textile fabrics, it will help open a new path for the high-value and efficient utilization of reed resources.

Cellulose acetate (CA) is a cellulose derivative prepared through the acetylation reaction of green and renewable cellulose. It has extensive industrial applications due to its low cost, non-toxicity, degradability and biocompatibility, such as coatings, cigarette filter materials, textile fibers, filter mem-

†To whom correspondence should be addressed.
20846@hnie.edu.cn, ORCID 0000-0002-4825-8903

branes, composite materials and biomedical products.[6-8] Acetate fiber made from CA has the characteristics of non-toxicity, strong adsorption capacity, good thermal stability and degradability.[9] The high-end textile fabrics woven from them have excellent moisture absorption, good drapeability, softness and comfort, easy dyeability, soft luster, and are similar to silk.[10] However, high-value-added acetate fibers have high performance requirements for raw material dissolving pulp, with an alpha cellulose content of more than 95%, whiteness higher than 90% and DP above 1000.[11] In addition to high-quality wood pulps and cotton linters, researchers have conducted extensive related research on the preparation of CA and acetate fibers using other biomass materials. Liu, *et al*.,[12] Cerqueira, *et al*.,[13] and Filho, *et al*.[14] used hemp, bagasse and recycled newspaper to prepare CA and optimized the process of acetylation reaction. He, *et al*.[15] prepared CA and acetate fibers using bamboo and comprehensively studied the pulp manufacturing process, synthesis of CA, as well as the spinning process, structure and properties of the acetate fibers. Hamed, *et al*.[16] extracted cellulose powder from olive industrial solid waste and converted it into high-value acetate fibers using pulping and multi-stage bleaching processes. Chen, *et al*.[17] used various cellulose raw materials such as microcrystalline cellulose, cotton linter pulp, wheat straw pulp, bamboo pulp, bleached softwood sulfite dissolving pulp and bleached hardwood kraft pulp to prepare acetate fibers by transesterification method, and studied the influence of raw material types on the properties of CA and acetate fibers. Andrade, *et al*.[18] used sorghum stalk as raw material to prepare high-purity and high-value acetate fibers by optimizing bleaching and acetylation reaction processes. Wu, *et al*.[19] used tobacco stalk dissolving pulp to prepare CA and further prepared micro/nano acetate fibers by electrostatic spinning method. However, there is currently a lack of research on preparing CA and acetate fibers from reed.

Based on previous research,[10] this study used self-made acetified grade triarrhena lutarioriparia (a kind of reed) dissolving pulp as raw material, concentrated sulfuric acid as catalyst and acetic anhydride as acetylating agent to prepare reed-based CA using the optimized process of homogeneous reaction method. The whiteness, degree of substitution (DS), degree of polymerization (DP), apparent morphology, chemical structure, crystal structure and thermal stability of CA were observed, tested and analyzed. This not only laid the foundation for preparing acetate fibers in the next step but also provided ideas for the transformation and reuse of reed as well as the development of high-value-added textiles.

Experimental

Materials. The experimental raw material was the self-made acetified grade triarrhena lutarioriparia dissolving pulp (TLDP), with an alpha cellulose content of 97.70%, whiteness of 91.42%, DP of 1413, pentosan content of 5.76%, ash content of 0.01% and iron content of 5.62 ppm. The chemical reagents used for

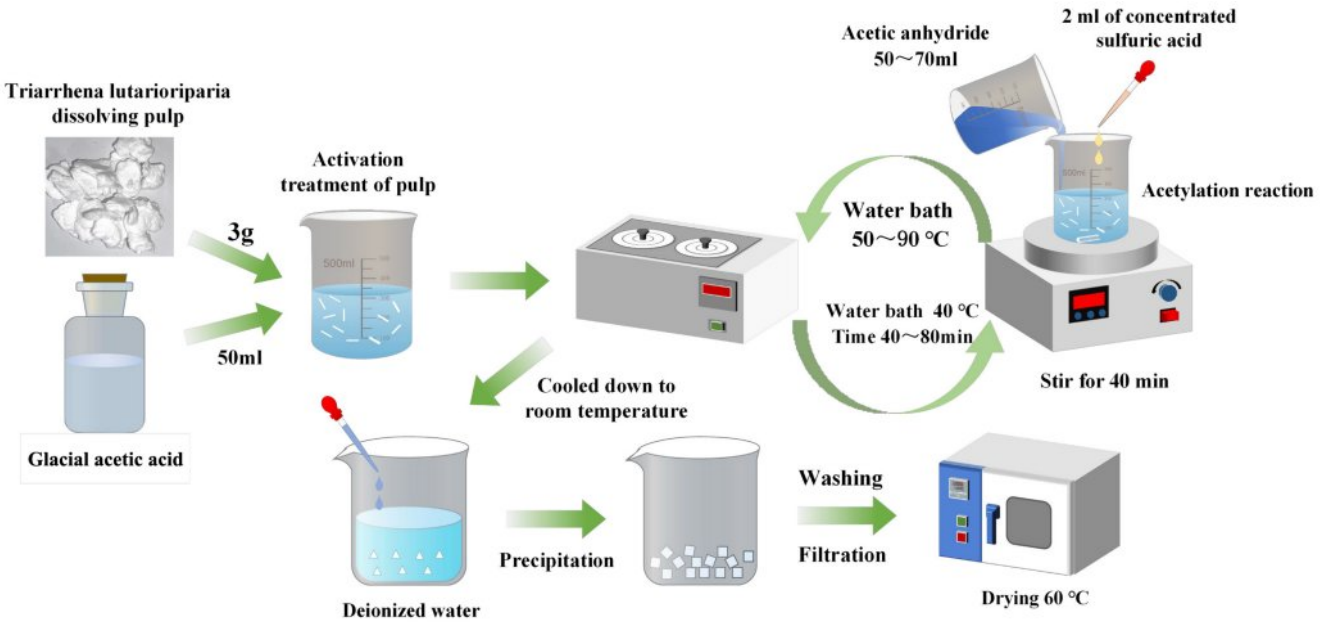

Figure 1. Preparation process of reed-based CA.

Table 1. $L_9(3^4)$ Orthogonal Experimental Design

Three levels	Three factors		
	A Activation time (min)	B Acetic anhydride dosage (mL)	C Reaction temperature (°C)
1	40	50	50
2	60	60	70
3	80	70	90

the experiment were purchased from China National Pharmaceutical Group Corporation, including acetic anhydride (CAS 108-24-7), glacial acetic acid (CAS 64-19-7), concentrated sulfuric acid (CAS 7664-93-9), dimethyl sulfoxide (CAS 67-68-5), phenolphthalein (CAS 77-09-8), sodium hydroxide (CAS 1310-73-2), dichloromethane (CAS 75-09-2) and methanol (CAS 67-56-1). Methyl sulfoxide-d6 was ordered from J&K Scientific (CAS 2206-27-1). Deionized water was prepared in the laboratory.

Preparation Process and Scheme of CA. The preparation process of reed-based CA is shown in Figure 1. First 3 g of dried dissolving pulp and 50 mL of glacial acetic acid were placed in a beaker and activated in a water bath at 40 °C for 40-80 min. Then, 50-70 mL of acetic anhydride was added to the beaker and stirred for 40 min before adding 2 mL of concentrated sulfuric acid for acetylation reaction at a water bath temperature of 50-90 °C. After the reaction, the mixture was naturally cooled to room temperature, then 150 mL of deionized water was added to precipitate white solids. After filtration, washing, and drying, CA was obtained.

An orthogonal experimental design method was used to explore the effects of activation time, reaction temperature and acetic anhydride dosage on the properties of CA. Table 1 shows the $L_9(3^4)$ orthogonal experimental design table with three factors and three levels.

Performance Testing and Characterization of CA. Whiteness: According to standard FZ/T 50013-2008, the blue light whiteness of CA was measured using an XT-48B/BN whiteness meter (Yante, China), with an average value obtained from five tests. Lighting conditions: D65 light source, wavelength of 457 nm, full width at half maximum (FWHM) of 44 nm.

DS: According to standard ISO 1597:2000, CA was dissolved in dimethyl sulfoxide, and then NaOH aqueous solution was added. The amount of alkali consumed during the hydrolysis of CA was determined by a titration method to calculate the hydrolyzed acetic acid yield, and DS was calculated using Equation (1).[12]

$$DS = 3.86C_{AV} / (142.86 - C_{AV}) \quad (1)$$

where DS represents the degree of substitution; C_{AV} represents the hydrolyzed acetic acid yield of CA, in g.

DP: According to standard ASTM D871-96, CA was dissolved in a mixed solvent of dichloromethane/methanol (9:1 w/w), and the intrinsic viscosity of the CA solution was measured using a Ubbelohde viscometer. The DP of CA was calculated using Equation (2).[15,20]

$$DP = 147\eta^{1.2} \quad (2)$$

where DP represents the degree of polymerization; η represents the intrinsic viscosity of CA, in dL/g.

Fourier Transform Infrared Spectroscopy (FTIR) Analysis: The FTIR spectra of TLDP and CA were recorded on a spectrometer model Tensor 27 (Bruker, Germany) by KBr pellet transmission method in the range of 4000~400 cm^{-1}.

X-ray diffraction (XRD) Analysis: The crystal structures of TLDP and CA were determined using an Aeris desktop X-ray diffractometer (Panalytical, Netherlands) with CuK_α radiation, voltage of 40 kV, current of 200 mA, scanning rate of 2°/min, step size of 0.02°, scanning range of 5°-90°.

Thermogravimetric Analysis - Derivative Thermogravimetri (TG-DTG) Analysis: The thermal stability of TLDP and CA was tested using a Mettler TGA/DSC 3+ thermogravimetric analyzer (Mettler Toledo, Switzerland) with nitrogen flow rate of 50 mL/min, temperature range of 30-600 °C, heating rate of 10 °C/min.

Apparent Morphology: The apparent morphology of TLDP and CA were observed using a TM4000 scanning electron microscope (Hitachi, Japan). The backscattered electron mode was used for observing images with an acceleration voltage of 10 kV.

Nuclear Magnetic Resonance (^{1}H NMR) Analysis: ^{1}H NMR spectrum of CA was measured by Routine NMR model Avance NEO 400 MHz (Brucker, Germany) with dimethyl sulfoxide-d_6 (DMSO-d_6) as solvent. All ^{1}H NMR experiments are reported in δ units.

Results and Discussion

Orthogonal Experimental Analysis. CA was prepared according to the $L_9(3^4)$ orthogonal experimental design. Its whiteness, DS and DP are shown in Table 2, and the range analysis results for each property are shown in Figure 2. Higher performance

Table 2. Orthogonal Experimental Results

No.	A Activation time (min)	B Acetic anhydride dosage (mL)	C Reaction temperature (°C)	Whiteness	DS	DP
1	40	50	50	83.14	2.53	162
2	40	60	70	84.24	2.61	172
3	40	70	90	81.28	2.47	156
4	60	60	90	80.92	2.55	159
5	60	70	50	82.63	2.51	161
6	60	50	70	84.67	2.57	165
7	80	70	70	81.96	2.49	158
8	80	50	90	80.86	2.42	154
9	80	60	50	85.15	2.56	168

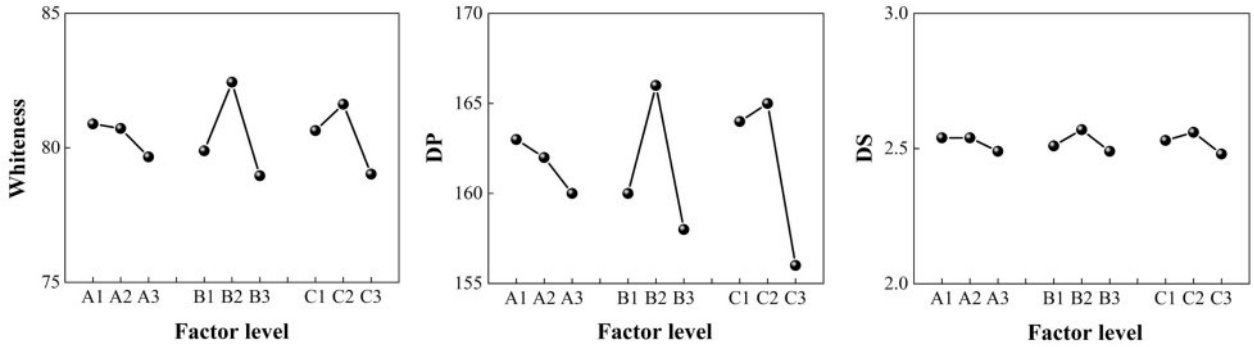

Figure 2. Range analysis of whiteness, DS and DP of CA.

Table 3. ANOVA of Whiteness

Source	Sum of squares	*df*	Mean square	*F*	*p*	Sig.
A	2.71	2	1.335	3.30	0.233	
B	19.47	2	9.735	23.70	0.040	*
C	10.37	2	5.185	12.65	0.073	(*)
Error	0.82	2	0.410			
Total	33.37	8				

Table 4. ANOVA of DS

Source	Sum of squares	*df*	Mean square	*F*	*p*	Sig.
A	0.005	2	0.003	10.00	0.106	
B	0.012	2	0.006	20.00	0.049	*
C	0.009	2	0.005	16.67	0.061	(*)
Error	0.0006	2	0.0003			
Total	0.0266	8				

is more conducive to meet the spinning requirements of acetate fiber. Considering comprehensively, the order of importance of the three factors and their optimal combination are B2C2A1, which means that acetic anhydride dosage is 60 mL, reaction temperature is 70 °C and activation time is 40 min.

The analysis of variance (ANOVA) results for the effects of

Table 5. ANOVA of DP

Source	Sum of squares	*df*	Mean Square	*F*	*p*	Sig.
A	16.67	2	8.335			
B	104.00	2	52.000	5.89	0.064	(*)
C	130.67	2	65.335	7.40	0.045	*
Error	18.67	2	9.335			
Error (A, e)	35.34	4	8.835			
Total	270.01	8				

Note: *Indicates a significant influence ($P < 0.05$), (*) indicates a certain influence ($0.05 \le P < 0.10$).

the three factors on whiteness, DS and DP of CA are shown in Table 3, Table 4 and Table 5, respectively. From the tables, Factor B has a significant influence on the whiteness and DS of CA and a certain influence on the DP. Factor C has a significant influence on the DP and a certain influence on the whiteness and DS. Factor A has no significant influence on DS, whiteness, or DP. Considering comprehensively, the order of importance of the three factors in influencing the three properties of CA is consistent with the range analysis results, which is B2C2A1. The final prepared CA sample exhibited performance parameters of whiteness 84.24, DP 172, and DS 2.61. In comparison with the CA extracted from waste newspapers by Filho, *et al.*[14] (DS 2.79) and the CA prepared from ramie fibers by Liu, *et al.*[12] (DS 2.5), the results of this study fall within a reasonable range, thereby adequately validating the feasibility of the process route.

Apparent Morphology. The apparent morphology of TLDP and CA are shown in Figure 3. As can be seen from Figure 3(a) and 3(b), the cellulose fibers in TLDP are long cylinders, covered with numerous grooves, holes and fine filaments, as shown by the red arrow in the figure. The uneven surface and holes increase the specific surface area of the pulp, facilitating the removal of lignin and hemicellulose, as well as the contact and reaction with acetylation reagents.[21] In addition, the pulp also contains some flattened wall cells with elliptical-shaped end. CA in Figure 3(c) has a rough surface and a high specific surface area, which is similar to the CA prepared by ramie fiber, sorghum straw and bamboo.[11,17,22] Figure 3(d) shows the commercially available wood-based CA with uneven surface and stringy filaments, which is different from the reed-based CA.

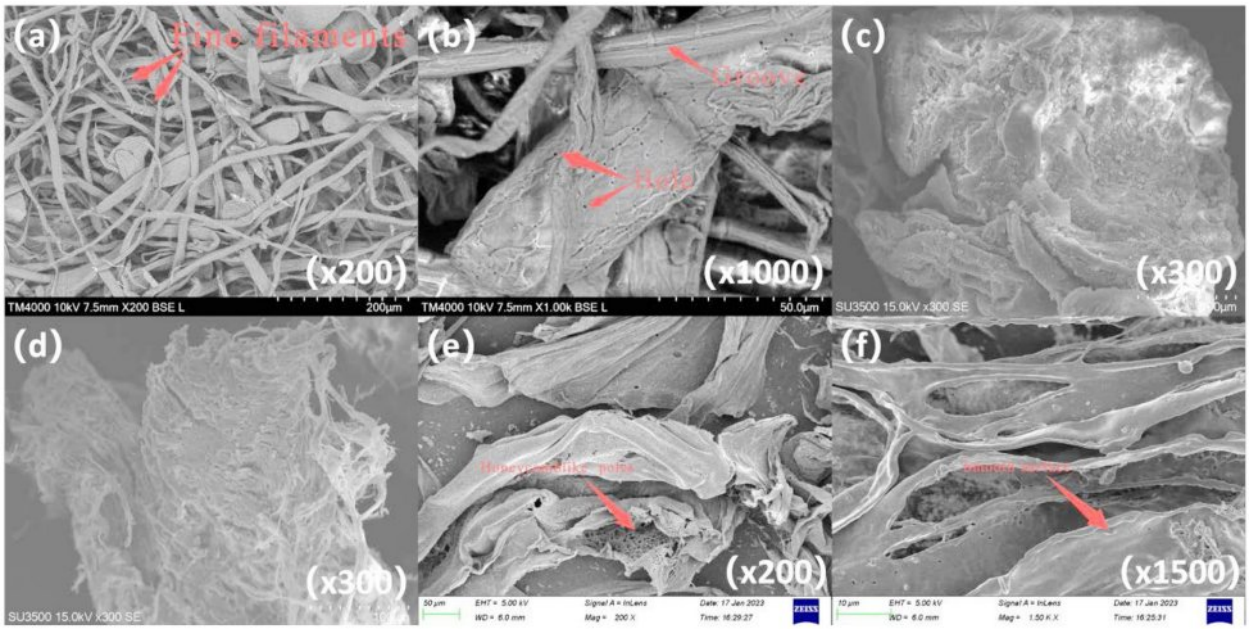

Figure 3. Apparent morphology of TLDP and CA: (a) cellulose fibers in TLDP with fine filaments; (b) cellulose fibers in TLDP with holes and grooves; (c) reed-based CA; (d) commercially available wood-based CA; (e) reed-based CA with honeycomb-like porous structure; (f) reed-based CA with smooth surface.

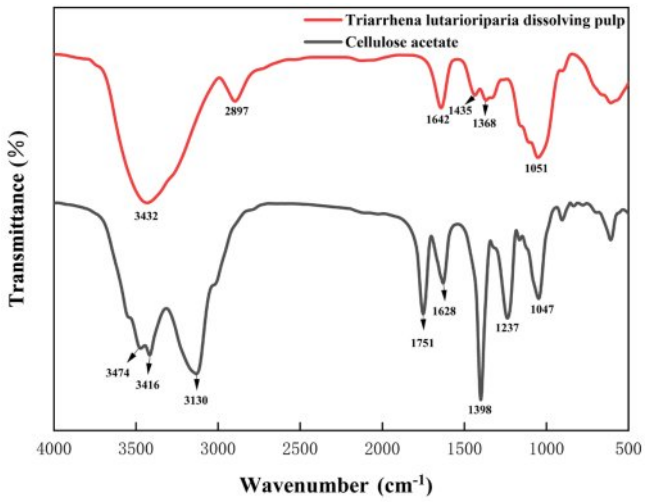

Figure 4. FTIR of TLDP and CA.

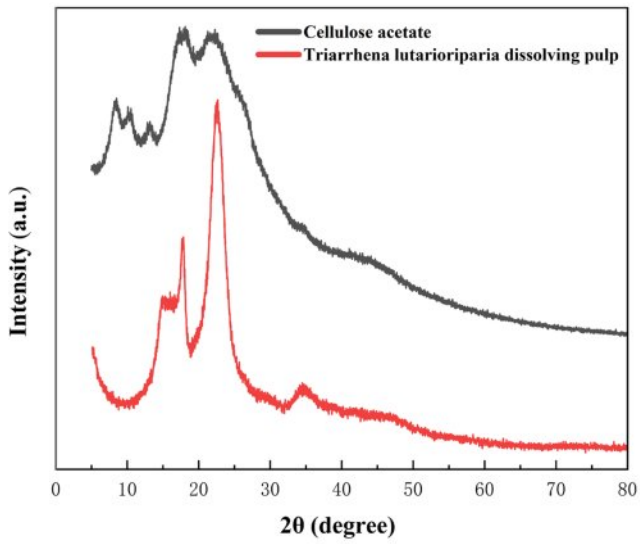

Figure 5. XRD curves of TLDP and CA.

In addition, CA in Figure 3(e) and 3(f) presents a relatively smooth surface and exhibits a partially honeycomb-like porous structure with varying sizes and uneven distribution, as shown by the red arrow in the figure.

Fourier Transform Infrared Spectroscopy (FTIR). Figure 4 shows the FTIR spectra of TLDP and CA. From Figure 4, it can be observed that TLDP exhibits typical peaks characteristic of cellulose, where 1051 cm^{-1} is the stretching vibration peak of C-O in the cellulose pyranose ring, 1368 cm^{-1} is the C-H bending vibration peak,[10,12] 1435 cm^{-1} is the bending vibration peak of -CH_2, 1642 cm^{-1} is attributed to the bending vibration peak of adsorbed water in the sample, 2897 cm^{-1} is the stretching vibration peak of methylene -CH_2, and 3432 cm^{-1} is the stretching vibration peak of hydroxyl group -OH.[23,24] Acetylated TLDP exhibits typical peaks characteristic of CA, where 1751 cm^{-1} is the stretching vibration peak of C=O, confirming the presence of ester groups. The stretching vibration peak of -CO- in the acetyl group at 1237 cm^{-1} further indicates the occurrence of acetylation reaction. The decreased absorption intensity of -OH in the range of 3416 to 3474 cm^{-1} suggests that most of the -OH groups on the cellulose macromolecular chain have been replaced by acetyl groups.[25,26]

XRD. Figure 5 shows the XRD patterns of the TLDP and CA. TLDP exhibits typical diffraction peaks of cellulose I, with characteristic peaks at 16.7°, 22.3° and 34.4°, consistent with the XRD curve of cotton fibers.[27] The high temperature and chemical agents during the pulping process disrupt the stable lignin-carbohydrate composite (LCC) structure in the raw material, causing degradation of cellulose and a corresponding decrease of its DP, which increases the accessibility of chemical agents to the pulp, thus facilitating the subsequent acetylation reaction. The acetylated TLDP not only changed the chemical composition, but also changed the crystal structure, and exhibited a typical diffraction curve of CA, with characteristic peaks at 8.5°, 10.6°, 13°, 18°, and 22.28°. The intensity of the diffraction peaks of CA is relatively weak, indicating a lower degree of crystallinity. This is because during the acetylation reaction, most of the hydroxyl groups on the cellulose macromolecular chains are substituted by larger acetyl groups, increasing the distance between macromolecular chains and breaking the intermolecular and intramolecular hydrogen bonds, resulting in the destruction of the stable structure of cellulose.[17,28]

TG-DTG. Figure 6 shows the TG-DTG curves of TLDP and CA. TLDP lost 8.4% of its mass between 30 °C and 130 °C

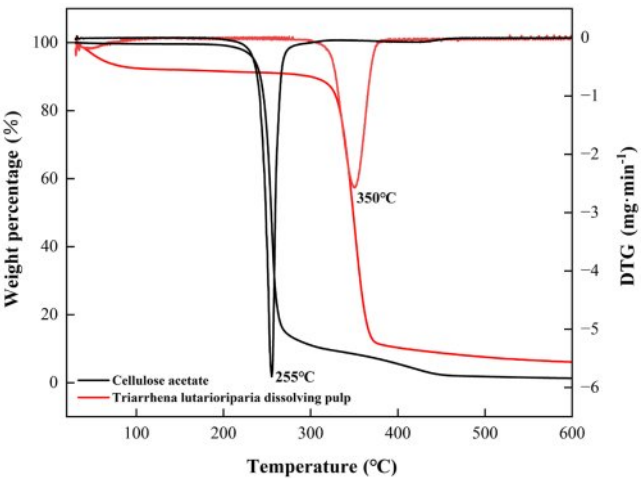

Figure 6. TG-DTG curves of TLDP and CA.

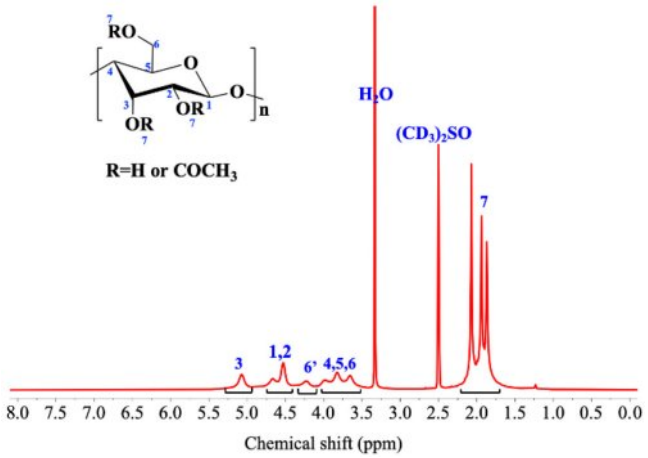

Figure 7. ^{1}H NMR of CA.

due to moisture evaporation. In the range of 130 °C to 600 °C, thermal decomposition became the main stage, with a mass loss of up to 85.97%, reaching its maximum at 350 °C. The residual carbon content after 600 °C was 6%. The mass of CA remained basically unchanged before 180 °C. The main stage of thermal decomposition of CA occurred between 180 °C and 450 °C, with a mass loss of 98.3%, reaching its maximum at 255 °C. During the period from 180 °C to 600 °C, the crystalline region of CA was completely destroyed and decomposed.[29,30] After the acetylation reaction, the hydroxyl groups in the cellulose macromolecular chain of TLDP were replaced by acetyl groups, reducing the crystallinity of CA and weakening its resistance.

^{1}H NMR. ^{1}H NMR of CA is shown in Figure 7. Signals at δ of 1.83 to 2.12 ppm belonging to three methyl protons of acetyl group appeared, confirming the hydroxyl groups were acetylated successfully and the formation of target CA as designed. Chemical shifts in the range of 3.40 to 5.50 belonging to seven protons of anhydro-glucose unit. Chemical shifts and integration of the seven protons and the methyl protons are consistent with those reported in the literature.[31,32] ^{1}H NMR (400 MHz, $(CD_3)_2SO$, δ(ppm)): 1.83-2.12(t, 9H), 3.40-4.08(t, 3H), 4.11-4.36(s, 1H), 4.39-4.82(d, 2H), 4.91-5.50(s, 1H).

Conclusion

Based on the self-made acetified grade TLDP, this study used an orthogonal experimental design to prepare CA in a glacial acetic acid/acetic anhydride/concentrated sulfuric acid reaction system. The optimal properties of CA were achieved when the acetic anhydride dosage was 60 mL, the reaction temperature was 70 °C and the activation time was 40 min, with a whiteness of 84.24, a DP of 172 and a DS of 2.61. After the acetylation reaction, the hydroxyl groups in the cellulose macromolecular chains were substituted by acetyl groups, resulting in the destruction of the stable structure of cellulose. Compared to TLDP, CA had a lower degree of crystallinity and weaker resistance to thermal decomposition. The successful preparation of reed-based CA with excellent properties not only laid the foundation for the next step of preparing acetate fibers but also provided insights for the transformation and reuse of reed as well as the development of high-value-added textiles.

Acknowledgments: This study was supported by Key Research and Development Program of Hunan Province (Grant No. 2022NK2042), Innovation Platform Project of Hunan Education Department (Grant No. 20K037), Science and Technology Innovation Double "50" Project of Xiangtan City, Hunan Province (Grant No. CG-YB20211002), Graduate Student Research and Innovation Project of Hunan Province (Grant No. CX20231281).

Conflict of Interest: The authors declare that there is no conflict of interest.

References

1. Wan, X. J. Study on the Comprehensive Utilization of Reeds in the South Dongting Lake Area. *Agr. Technol. Eq.* **2019**, 356, 87-88.
2. Zhao, Y. Y.; Lu, X. T.; Liu, X.; Liu, M. Y. Effect of Reed Straw on the Performance of Recycled Brick Aggregate Concrete and Evaluation of Economic Benefits. *Constr. Build. Mater.* **2024**, 411, 134205.
3. Zhang, Z. P.; Zhu, L. T.; Lu, J.; Zhu, B. W.; Pan, Q. W.; Cheng, Y.; Tao, Y. H.; Du, J.; Wang, H. S. Integrating Surfactants with Low Enzyme Loading to Increase the Glucan Conversion and Ethanol Concentration of Reed after Combined Pretreatment. *Ind. Crop Prod.* **2023**, 204, 117360.
4. Li, X. Y.; Wang, M.; Wen, B. L.; Zhang, Q. L.; Chen, J. Z.; Li, X. J.; An, Y. Reed-mush-room-fertilizer Ecological Agriculture in Wetlands: Harvesting Reed to Cultivate Mushroom and Returning Waste Substrates to Restore Saline-alkaline Marshes. *Sci. Total Environ.* **2023**, 878, 162987.
5. Ascacio-Valdés, A.; De León-Medina, J. C.; De León-Zapata, M. A.; Laredo-Alcalá, E. I.; Flores-Gallegos, A. C.; Meléndez-Rentería, N. P. Sustainable Use of Giant Reed to Produce Industrialized Enzymes. *Heliyon* **2023**, 9, e18748.
6. Dong, G. P.; Yuan, Z. Q.; Guo, X. J. Functional Properties of Nano-SiO_2/pinewood-derived Cellulose Acetate Composite Film

for Packaging Application. *Ind. Crop Prod.* **2023**, 204, 117253.
7. Rafique Khan, M.; Liao, S. Q.; Farooq, A.; Naeem M, A.; Wasim, M.; Wei, Q. F. Regeneration and Modification of Cellulose Acetate from Cigarette Waste: Biomedical Potential by Encapsulation of Tetracycline Hydrochloride. *Int. J. Biol. Macromol.* **2023**, 250, 126266.
8. Oprea, M.; Voicu, S. I. Cellulose Acetate-based Membranes for the Removal of Heavy Metals from Water in the Context of Circular Economy. *Ind. Crop Prod.* **2023**, 206, 117716.
9. Du, Z. J.; Xu, Y.; Wei, Q. F.; Chen, Y. Preparation and Characterization of Porous Diacetate Fiber. *Polym. Mater. Sci. Eng.* **2018**, 34, 108-113.
10. Wang, X. K.; Xie, K. F.; Zhou, H. S.; Bao, X. J.; Xu, Y. S. Preparation and Characterization of Acetate Grade Reed Dissolving Pulp. *J. Text. Res.* **2023**, 44, 52-59.
11. Saka, S.; Matsumura, H. Wood Pulp Manufacturing and Quality Characteristics. *Macromol. Symp.* **2004**, 208, 37-48.
12. Liu, Z. T.; Fan, X. S.; Wu, J.; Zhang, L. L.; Song, L. P.; Gao, Z. W.; Dong, W. S.; Xiong, H. P.; Peng, Y. D.; Tang, S. W. A Green Route to Prepare Cellulose Acetate Particle from Ramie Fiber. *React. Funct. Polym.* **2007**, 69, 104-112.
13. Cerqueira, D. A.; Filho, G. R.; Meireles, C. S. Optimization of Sugarcane Bagasse Cellulose Acetylation. *Carbohydr. Polym.* **2007**, 69, 579-582.
14. Filho, G. R.; Monteiro, D. S.; Meireles, C. S.; Meireles, C. D. S.; Assunção, R. M. N.; Cerqueira, D. A.; Barud, H. S.; Ribeiro, S. J. L.; Messadeq, Y. Synthesis and Characterization of Cellulose Acetate Produced from Recycled Newspaper. *Carbohyd. Polym.* **2008**, 73, 74-82.
15. He, J. X. Preparation of High-grade Bamboo Dissolving Pulp and Its Application for the Synthesis of Cellulose Acetate. *Degree Thesis*, Donghua University (Shanghai), July, 2007.
16. Hamed, O. A.; Jodeh, S.; Al-Hajj, N.; Hamed, E. M.; Abo-Obeid, A.; Fouad, Y. Cellulose Acetate from Biomass Waste of Olive Industry. *J. Wood Sci.* **2015**, 61, 45-52.
17. Chen, J. H.; Xu, J. K.; Wang, K.; Cao, X. F.; Sun, R. C. Cellulose Acetate Fibers Prepared from Different Raw Materials with Rapid Synthesis Method. *Carbohydr. Polym.* **2016**, 137, 685-692.
18. Andrade, A. J. A.; Lisboa dos Santos, M. D.; Morais, C. C.; Ramirez Ascheri, J. L.; Signni, R.; dos Santos, D. M.; Cavalcante Bastos, S. M.; Ramirez Ascheri, D. P. Sorghum Straw: Pulping and Bleaching Process Optimization and Synthesis of Cellulose Acetate. *Int. J. Biol. Macromol.* **2019**, 135, 877-886.
19. Wu, J. J.; Qin, X. H. Preparation and Characterization of Cellulose Acetate Sub-micro Fiber from Burley Tobacco Stalk Pulp. *J. Text. Res.* **2019**, 40, 1-8.
20. Gao, L. B.; Zhang, S. Y.; Shi, S.; Ling, C.; Wang, B. W. Synthesis, Structure and Properties of Cellulose Acetate. *Appl. Chem. Ind.* **2020**, 49, 55-59.
21. He, J. X.; Cui, S. Z.; Wang, S. Y. Preparation and Crystalline Analysis of High-Grade Bamboo Dissolving Pulp for Cellulose Acetate. *J. Appl. Polym. Sci.* **2008**, 107, 1029-1038.
22. Cai, J.; Zhou, R.; Li, T. T.; He, J. R.; Wang, G. Z.; Wang, H. B.; Xiong, H. G. Bamboo Cellulose-Derived Cellulose Acetate for Electrospun Nanofibers: Synthesis, Characterization and Kinetics. *Cellulose* **2018**, 25, 391-398.
23. Andreeva, O. A.; Burkova, L. A.; Grebenkin, A. N.; Grebenkin, A. A. IR Spectroscopic Study of Prepurified Flax. *Russ. J. Appl. Chem*. **2002**, 75, 1513-1516.
24. Ali, S.; Khatri, Z.; Oh, K. W.; Kim, I. S.; Kim, S. H. Zein/Cellulose Acetate Hybrid Nanofibers: Electrospinning and Characterization. *Macromol. Res.* **2014**, 22, 971-977.
25. Schilling, M.; Bouchard, M.; Khanjian, H.; Learner, T.; Phenix, A.; Rivenc, R. Application of Chemical and Thermal Analysis Methods for Studying Cellulose Ester Plastics. *Acc. Chem. Res.* **2010**, 43, 888-896.
26. Chen, X. M.; Zou, H. F.; Ni, J. Y.; Shun, F. Synthesis and Characteristics of Composite Chiral Stationary Phases Based on Cellulose Derivatives. *J. Sep. Sci.* **2003**, 26, 29-36.
27. Yakunin, N. A.; Zavadskii, A. E. Effect of Dampening on the Supramolecular Structure of Cotton Cellulose. *Fibre Chem*. **2004**, 36, 463-466.
28. Fan, G. Z.; Wang, M.; Liao, C. J.; Fang, T.; Li, J. F.; Zhou, R. Isolation of Cellulose from Rice Straw and Its Conversion into Cellulose Acetate Catalyzed by Phosphotungstic Acid. *Carbohydr. Polym.* **2013**, 94, 71-76.
29. Yang, Z. P.; Xu, S. W.; Ma, X. L.; Wang, S. Y. Characterization and Acetylation Behavior of Bamboo Pulp. *Wood Sci. Technol.* **2008**, 42, 621-632.
30. Das, A. M.; Ali, A. A.; Hazarika, M. P. Synthesis and Characterization of Cellulose Acetate from Rice Husk: Eco-Friendly Condition. *J. Carbohydr. Polym.* **2014**, 112, 342-349.
31. Biswas, A.; Saha, B. C.; Lawton, J. W.; Shogren, R. L.; Willett, J. L. Process for Obtaining Cellulose Acetate from Agricultural By-Products. *Carbohydr. Polym.* **2006**, 64, 134-137.
32. Xiao, W. H.; Liu, R. Z.; Zhao, G. L.; Guo, D. Y.; Yang, Y. F.; Zhou, C. F. Preparation of Cellulose Triacetate from Corn Stover Cellulose by Trifluoroacetic Acid. *Trans. Chin. Soc. Agric Mach.* **2021**, 52, 331-337.